Overflow Characteristics of Circular Weirs: Effects of Inflow Conditions

By H. Chanson[1] and J. S. Montes[2]

Abstract: The most common types of weirs are the broad-crested weir, the sharp-crested weir, the circular-crested weir, and nowadays, the ogee crest weir. Advantages of the cylindrical weir shape include the stable overflow pattern, the ease to pass floating debris, the simplicity of design compared to ogee crest design, and the associated lower costs. In this study, the writers describe new experiments of circular weir overflows, with eight cylinder sizes, for several weir heights and for five types of inflow conditions: partially developed inflow, fully developed inflow, upstream ramp, upstream undular hydraulic jump, and upstream (breaking) hydraulic jump. Within the range of the experiments, the cylinder size, the weir height D/R and the presence of an upstream ramp had no effect on the discharge coefficient, flow depth at crest, and energy dissipation. But the inflow conditions had substantial effects on the discharge characteristics and flow properties at the crest. Practically, the results indicate that discharge measurements with circular weirs are significantly affected by the upstream flow conditions.

INTRODUCTION

Waters flowing over weirs and spillways are characterized by a rapidly varied flow region near the crest. The most common types of weir crest are the broad-crested weir, the sharp-crested weir, the circular-crested weir, and nowadays, the ogee crest weir. Advantages of the circular weir shape (Figs. 1 and 2) are the stable overflow pattern compared to sharp-crested weirs, the ease to pass floating debris, the simplicity of design compared to ogee crest design, and the associated lower cost. Circular-crested weirs have larger discharge capacity (for identical upstream head) than broad-crested weirs and sharp-crested weirs.

Related applications include roller gates and inflated flexible membrane dams (i.e., rubber dams). Roller gates (also called cylindrical gates or rolling dams) are hollow metal cylinders held in place by concrete piers, and they can be raised to allow the flow underneath [e.g., Wegmann (1922); Petrikat (1958)]. For small overflows it is not economical to lift the gate and overflow is permitted. Inflated flexible membrane dams are a new form of weir. They are used to raise the upstream water level by inflating the rubber membrane placed across a stream or along a weir crest. Small overflows are usually allowed without dam deflation and the overflow characteristics are somehow similar to those of circular weirs [e.g., Anwar (1967); Chanson (1996)]. These related applications are nevertheless special areas of interest and need to be researched on their own.

In the present study, the characteristics of cylindrical weirs are reinvestigated and a particular emphasis is placed on the effect of the upstream flow conditions (Tables 1 and 2). The experimental setups are described in the next paragraph. The results are presented later and compared with previous studies (Fig. 3).

Bibliographic Review

Cylindrical weirs were common in the late 19th century and early 20th century prior to the introduction of the ogee shape. During the 19th century, developments in improving weir discharge capacity led to the design of circular-crested weirs, e.g., the work of H. E. Bazin, in France. (Henri Emile Bazin (1829–1917) was a French hydraulic engineer who worked with H. P. G. Darcy at the beginning of his career.) Although Bazin's work on weirs is best known for his accurate observations on sharp-crested weirs (Bazin 1888, 1890, 1891, 1894,

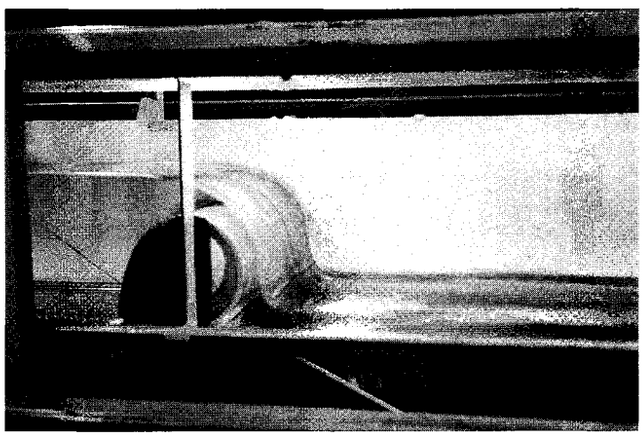

(a)

(b)

FIG. 1. Photographs of Overflow above Circular Weirs: (a) Side View of Cylinder No. 2 in Channel QII—Flow from Left to Right (q_w = 0.026 m²/s; W = 0.25 m; R = 0.0524 m; C_D = 1.35; HW/R = 1); (b) Top View of Cylinder No. 2 in Channel QII—Flow from Left to Right (Same Flow Conditions; Note Dye Injection Upstream of Cylinder on Channel Centerline)

[1]Sr. Lect., Fluid Mech., Hydr. and Envir. Engrg., Dept. of Civ. Engrg., The Univ. of Queensland, Brisbane QLD 4072, Australia.

[2]Sr. Lect., Dept. of Civ. and Mech. Engrg., Univ. of Tasmania, Hobart TAS 7000, Australia.

Note. Discussion open until November 1, 1998. To extend the closing date one month, a written request must be filed with the ASCE Manager of Journals. The manuscript for this paper was submitted for review and possible publication on June 18, 1997. This paper is part of the *Journal of Irrigation and Drainage Engineering*, Vol. 124, No. 3, May/June, 1998. ©ASCE, ISSN 0733-9437/98/0003-0152–0162/$8.00 + $.50 per page. Paper No. 16027.

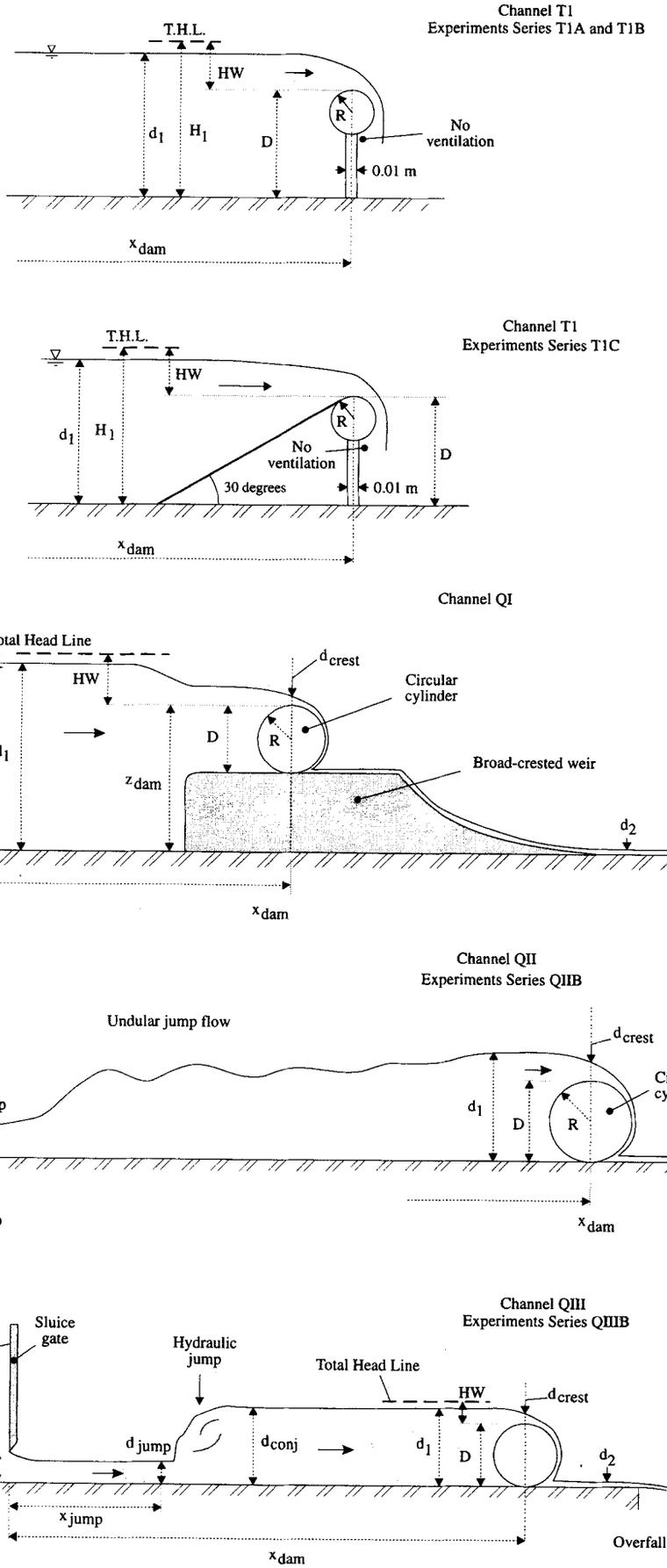

FIG. 2. Sketch of Experimental Channels

TABLE 1. Summary of Experimental Flow Conditions

Series (1)	Slope, α (degrees) (2)	q_w (m^2/s) (3)	d_1 (m) (4)	Weir height, D (m) (5)	Inflow conditions (6)	Remarks (7)
(*a*) Channel T1: Horizontal channel (W = 0.301 m; x_{dam} = 8 m)						
T1A and T1B	0				Partially developed inflow and fully developed inflow	Vertical perspex support (10 mm thick)
		0.011 to 0.074	0.193 to 0.362	0.154, 0.204, and 0.254		Cylinder no. A
		0.008 to 0.071	0.183 to 0.352	0.154, 0.204, and 0.254		Cylinder no. B
		0.011 to 0.076	0.194 to 0.359	0.154, 0.204, and 0.254		Cylinder no. C
		0.001 to 0.072	0.181 to 0.359	0.154, 0.204, and 0.254		Cylinder no. D
T1C	0				Ramp	30° upstream ramp
		0.003 to 0.073	0.173 to 0.3565	0.154, 0.204, and 0.254		Cylinder no. A
		0.006 to 0.072	0.183 to 0.3545	0.154, 0.204, and 0.254		Cylinder no. B
		0.005 to 0.075	0.176 to 0.3535	0.154, 0.204, and 0.254		Cylinder no. C
		0.005 to 0.073	0.185 to 0.3495	0.154, 0.204, and 0.254		Cylinder no. D
(*b*) Channel QI: Broad-crested weir channel (Δz = 0.0645 m; W = 0.25 m; x_{dam} = 1.2 m)						
QI	0				Weir and partially developed flow	Cylinder located on a weir crest
		0.0005 to 0.005	0.154 to 0.172	0.835		
(*c*) Channel QII: Long tilting flume (W = 0.25 m; x_{dam} = 11 m)						
QIIA	0.191				Fully developed inflow	Mild slope experiments
		0.0008 to 0.04	0.09 to 0.15	0.0835		Cylinder no. 1
		0.0008 to 0.12	0.11 to 0.23	0.1048		Cylinder no. 2
		0.002 to 0.06	0.16 to 0.235	0.1509		Cylinder no. 3
		0.0009 to 0.004	0.24 to 0.25	0.2332		Cylinder no. 4
QIIB	0.191 to 0.97				Upstream undular hydraulic jump	Steep slope experiments; undular hydraulic jump upstream of weir
		0.004 to 0.040	0.096 to 0.151	0.0835		Cylinder no. 1
		0.085 to 0.035	0.127 to 0.169	0.1048		Cylinder no. 2
(*d*) Channel QIII: Horizontal channel (W = 0.25 m; x_{dam} = 2.55 m)						
QIIIA	0				Partially developed inflow	Sluice gate fully opened
		0.0013 to 0.027	0.24 to 0.30	0.2332		Cylinder no. 4
QIIIB	0				Upstream hydraulic jump	Hydraulic jump upstream of weir
		0.05 to 0.14	0.186 to 0.254	0.1048		Cylinder no. 2; sluice gate openings: 0.02, 0.03, 0.04, 0.05, 0.065, and 0.08 m

Note: W = channel width; x_{dam} = longitudinal distance from the cylinder axis to the channel intake. Cylinder characteristics are described in Table 2.

TABLE 2. Cylindrical Weir Characteristics

Cylinder number (1)	Reference radius, $R(^+)$[a] (m) (2)	Remarks (3)
A	0.07905	Cylinder made of PVC pipe.
B	0.0671	Cylinder made of PVC pipe.
C	0.05704	Cylinder made of PVC pipe.
D	0.0290	Cylinder made of PVC pipe.
1	0.04175	Cylinder built in concrete with a hollow core.
2	0.0524	Cylinder built in concrete with a hollow core.
3	0.07544	Cylinder built in concrete with a hollow core.
4	0.1166	Cylinder built in concrete with a hollow core.

[a]$(^+)$ = curvature radius at crest.

1896, 1898), which were used later by Creager to develop his ogee crest profile (Creager 1917), he also conducted investigations in round-crested profiles, later applied in the design of the Pont Dam in French Burgundy. Nowadays most crests have an ogee shape [e.g., Creager profile, Scimemi profile, Scimemi (1930)].

Major studies of circular weirs include Rehbock (1929), Fawer (1937), and Sarginson (1972). These investigations showed that the discharge coefficient C_D was close to and usually larger than unity, and C_D was primarily a function of the ratio of upstream head to crest radius HW/R, C_D increasing with increasing values of HW/R, where HW is the total head above crest and R is the crest curvature radius.

Two studies (Escande and Sananes 1959; Rouve and Indlekofer 1974) investigated particularly the effects of nappe suction and nappe ventilation on the discharge characteristics. Both investigations showed that nappe suction prevented flow separation and led to larger discharge coefficients by up to 15 to 20% (Escande and Sananes 1959). A recent PhD thesis (Vo 1992) provided new information on the velocity field at and downstream of the crest. The results suggested that the flow field may be predicted by ideal-fluid flow theory.

EXPERIMENTAL APPARATUS AND METHOD

The overflow characteristics of cylindrical weirs were investigated in the laboratory for several configurations, i.e., eight cylinder sizes ($0.029 < R < 0.117$ m), several weir heights ($2 < D/R < 9$), and several types of inflow conditions: fully developed, partially developed, upstream ramp, upstream hydraulic jump, and upstream undular hydraulic jump (Tables 1 and 2).

Four channels of rectangular cross sections were used (Fig. 2). Each flume is supplied with recirculating water supplied by a constant head tank. All cylindrical weirs were smooth (PVC or winding-varnish surface) and the downstream face of the cylinders was not ventilated in all the experiments.

The water discharge was measured either by a volume-to-

Reference (1)	C_D (2)	Comments (3)
REHBOCK (1929)	$0.552 + 0.177 * \sqrt{30 - \left(5 - \frac{HW}{R}\right)^2}$	Model data as given in SARGINSON (1972).
FAWER (1937)	$1 + 0.221*\frac{HW}{R} - 0.0260*\left(\frac{HW}{R}\right)^2$	Model data. W = 0.303 m. R = 0.0325 m. 0.5 ≤ HW/R ≤ 3. 0 ≤ D-R ≤ 0.3325 m.
JAEGER (1956)	$\frac{3}{2} * \left(\frac{R}{HW} + \frac{4}{3} - \sqrt{\left(\frac{R}{HW}\right)^2 + \frac{4}{3} * \frac{R}{HW}}\right)$	Theoretical result validated with model data.
MATTHEW (1963)	$1 + 0.230*\frac{HW}{R} - 0.010*\left(\frac{HW}{R}\right)^2 - 0.0154*\frac{R}{HW}$	Model data. Vertical upstream face. R = 0.0254 m. 0.1 ≤ HW/R ≤ 1.
	$1 + 0.240*\frac{HW}{R} - 0.028*\left(\frac{HW}{R}\right)^2 - 0.0184*\frac{R}{HW}$	Upstream face with 45-degree slope. R = 0.0254 m. 0.1 ≤ HW/R ≤ 1.
	$1 + 0.240*\frac{HW}{R} - 0.026*\left(\frac{HW}{R}\right)^2 - 0.0181*\frac{R}{HW}$	Upstream face with 45-degree slope. R = 0.0254 m. 0.1 ≤ HW/R ≤ 1. D=2*R.
MONTES (1964)	$1.169 * \left(\frac{HW}{R}\right)^{1/8}$	Re-analysis of data. 0.05 < HW/R < 1.2
SARGINSON (1972)	$0.702 + 0.145*\sqrt{33 - \left(5.5 - \frac{HW}{R}\right)^2} - 3.146*\frac{\sigma}{\rho_w*g*HW}*\left(1 - \left(1 + 1.2*\frac{HW}{R}\right)^{-4/9}\right) + 0.160*\frac{HW}{D}$	Model data. Ventilated nappes. Liquids : water, water + Lissapol N ($0.034 < \sigma < 0.059$ N/m). R = 0.00315 to 0.068 m. HW/R < 2 to 4
ROUVE and INDLEKOFER (1974)	$0.94440 + 0.35497*\frac{HW}{R} - 0.10791*\left(\frac{HW}{R}\right)^2 + 0.010309 * \left(\frac{HW}{R}\right)^3$	Model data. Semicircular crest with ventilated nappe. W = 0.599 m. 0.0102 ≤ R 0.148 m. 0.21 ≤ D-R ≤ 0.96 m. for HW/R < 4.0
	1.299	for HW/R > 4.0
PRESENT STUDY	$C_D = 1.2676 * \left(\frac{HW}{R}\right)^{0.1811}$	Model data. Un-ventilated nappes. W = 0.25 to 0.3 m. Horizontal channels. Partially-developed inflow. 0.35 < HW/R < 3.5
	$C_D = 1.1854 * \left(\frac{HW}{R}\right)^{0.1358}$	Fully-developed inflow. 0.45 < HW/R < 1.9

Note : HW : head above weir crest; R : crest radius of curvature.

FIG. 3. Empirical Formulas of Discharge Coefficients above Circular-Crested Weirs (Laboratory Studies and Theoretical Results)

time method using a calibrated 300-L tank (channels QI and QII) or by a 90° V-notch weir (channels T1 and QIII). The percentage of error is expected to be less than 5%. The flow depths were measured using point gauges. The error on the flow depth was 0.2 mm in channel T1 and less than 0.1 mm in channels QI, QII, and QIII equipped with a Mitutoyo digimatic caliper (Ref. No. 500-171). The error on the longitudinal position was $\Delta x < 1$ mm. In addition photographs were taken during the experiments and used to visualize the flow patterns.

Full details of the experimental apparatus and of the data were reported in Chanson and Montes (1997).

Experimental Procedures

Series T1A and T1B experiments investigated the discharge characteristics of cylindrical weirs in a horizontal channel with various support heights, and the inflow conditions were partially developed and fully developed. T1C experiments studied particularly the effects of a 30° upstream ramp. Series QI experiments described the overflow of a cylindrical weir located on a broad-crested weir. Series QIIA experiments were performed in a long tilting flume with fully developed upstream flow and with a mild slope. Series QIIB experiments were performed in the same channel QII with steep slopes, and an undular hydraulic jump took place upstream of the weir. Series QIIIA experiments studied the characteristics of the largest cylinder with partially developed inflow. In the same flume, series QIIIB experiments investigated the effects of (breaking) hydraulic jumps upstream of a cylindrical weir. Altogether the writers performed over 385 new experiments (Chanson and Montes 1997).

Results

At a cylindrical weir (e.g., Fig. 1), the overflowing waters are subjected to a rapid change in streamline direction upstream of the weir, nappe adherence on the downstream face of the cylindrical weir, and nappe separation near the downstream bottom of the weir. Dye injection showed that the change of streamline direction occurs shortly upstream of the weir, i.e., at a distance of about one to two weir heights. The flow redistribution is sometimes associated with the development of helicoidal vortices with horizontal axis along the upstream base of the weir and by sidewall vortices of irregular shapes along the upstream face of the weir (near the sidewall).

As the waters pass over the dam crest, the nappe free-surface remains smooth and clear, and the falling nappe adheres

to the weir face. The nappe adherence process is a form of Coanda effect [named after Henri Coanda, Romanian scientist, who first patented it (Coanda 1932)]. It results from the modification of the pressure field within the nappe, caused by the convex invert curvature, inducing a suction pressure on the wall. Further, some fluid entrainment into the nappe is caused by turbulent mixing, and the induced flow (directed towards the nappe) leads to a force on the body normal to the flow direction (this process is also called Chilowsky effect). On the lower downstream quadrant of the cylinder, the nappe continues to adhere to the cylinder wall despite the gravity effect opposing the Coanda force (Fig. 1). Near the weir bottom, nappe separation takes place. Usually the nappe separation occurs at the weir bottom because of the presence of the channel bed or weir support.

At large ratio of head on crest to radius, nappe separation was observed on the downstream face of supported weirs (i.e., $D > 2R$). Such a separation occurred in absence of nappe ventilation. Sarginson (1972) and Vo (1992) observed a similar behavior with ventilated nappes.

DISCHARGE COEFFICIENT

Presentation

In open channels, maximum flow rate is achieved at critical flow conditions (Belanger 1828) and the maximum discharge per unit width at a weir crest equals

$$q_w = \sqrt{g}\left(\frac{2}{3}HW\right)^{3/2} \quad \text{for ideal fluid flow} \tag{1}$$

where g = gravity acceleration; and HW = upstream total head above the weir crest. Eq. (1) derives from the Bernoulli equation assuming hydrostatic pressure distribution at the crest and an uniform velocity distribution for a rectangular channel. In practice the observed discharge differs from (1) because the pressure distribution on the crest is not hydrostatic and the velocity distribution is not uniform [e.g., Vo (1992)]. Usually the flow rate is expressed as

$$q_w = C_D\sqrt{g}\left(\frac{2}{3}HW\right)^{3/2} \tag{2}$$

where C_D = discharge coefficient. It equals unity for an ideal broad-crested weir.

Experimental Results: General Trends

New experimental observations are reported in Figs. 4 to 6. The discharge coefficient data are plotted as functions of the ratio HW/R where R is the curvature radius of the crest.

The data show consistently an increase of the discharge coefficient with increasing dimensionless head above crest (Figs. 4 and 5). The data show also that the discharge coefficient is mostly larger than unity, i.e., for a given upstream head, the discharge on a circular weir is larger than that on a broad-crested weir.

For the range of the experiments (Table 1), the data analysis (Chanson and Montes 1997) indicate that the discharge coefficient is independent of the cylinder size (i.e., radius of curvature R) and of the dimensionless weir height D/R, and the presence of an upstream ramp has no effect on the discharge coefficient.

Further, the upstream flow conditions are extremely important and the type of inflow conditions affects substantially the overflow characteristics. With fully developed upstream flow conditions, the data shown in Fig. 4(a) are best fitted by

$$C_D = 1.185\left(\frac{HW}{R}\right)^{0.136} \quad \text{fully developed inflow } (0.45 < HW/R < 1.9) \tag{3}$$

with a coefficient of correlation of 0.972. For partially developed inflows, the data [Fig. 4(b)] are best correlated by

$$C_D = 1.1268\left(\frac{HW}{R}\right)^{0.181} \quad \text{partially developed inflow } (0.35 < HW/R < 3.5) \tag{4}$$

with a 0.984 normalized correlation coefficient. Both (3) and (4) are reported in Figs. 4 and 5.

Fig. 4 indicates that, for a given ratio HW/R, larger discharge coefficients are observed with fully developed inflow than with partially developed inflow. The result can be predicted analytically (Chanson and Montes 1997). Applying the Bernoulli equation along the free-surface streamline between the upstream flow location and the crest, the discharge coefficient can be expressed in terms of the upstream flow depth d_1, the flow depth at the crest d_{crest}, the weir crest height D, and the boundary layer characteristics. For an inflow with a developing bottom boundary layer, the Bernoulli equation yields

$$C_D = \frac{d_{crest}}{d_c}\sqrt{\frac{3\left(1 - \frac{2}{3}\frac{d_{crest}}{d_c}\right)}{k^2 - \frac{d_{crest}^2}{d_1^2}\left(\frac{N+1}{N+1-\frac{\delta}{d_1}}\right)^2}} \quad \text{partially developed inflow} \tag{5}$$

where δ = boundary layer thickness; k = constant of proportionality; $1/N$ = velocity distribution power law exponent; and d_c = critical flow depth in rectangular channel with hydrostatic pressure distribution (see Appendix I for full development). As the ratio d_{crest}/d_c is nearly independent of the upstream flow conditions (see next paragraph), (5) implies that C_D increases with increasing ratio δ/d_1 for given inflow conditions. That is, C_D is larger for fully developed inflow conditions (i.e., $\delta/d_1 = 1$) than for partially developed inflows (i.e., $\delta/d_1 < 0$).

Fig. 5 presents the discharge coefficient for the experiments series T1C with the 30° upstream ramp. The data are compared with (3) and (4), and show a broader scatter than for the experiments without ramp (Fig. 2). Overall the experimental results suggest that the upstream ramp has no or little effect on the discharge capacity of circular weirs. Previous studies [e.g., Matthew (1963); Vo (1992)] reported a similar conclusion. Although an upstream ramp does not improve the discharge coefficient, the ramp can facilitate the passage of large debris (e.g., ice or trees) and it must be recommended in natural streams where floating debris are common.

Effect of Upstream Hydraulic Jumps

The effects of an upstream hydraulic jump were investigated in two channels (QII and QIII). One series of experiments was performed with a breaking hydraulic jump upstream of the weirs (series QIIIB). Another series was performed with an upstream undular hydraulic jump (series QIIB).

In Fig. 6, the discharge coefficient data (for one cylinder size) are plotted as a function the dimensionless distance between an upstream hydraulic jump and the weir where $X = x_{dam} - x_{jump}$, and x_{dam} and x_{jump} are defined in Fig. 2. In Fig. 6, the limiting values of C_D for large values of X/D (i.e., no jump) are shown also. Fig. 6(a) shows experiments with an upstream undular jump ($F \leq 1.25$) and Fig. 6(b) presents experiments with an upstream breaking jump ($F > 3$). The results indicate consistently that the presence of an upstream undular jump tends to increase the discharge coefficient, and C_D increases with decreasing distance X/D for a given head on crest. And the presence of an upstream breaking jump induces a reduction in discharge coefficient [Fig. 6(b)]. Visually, the presence of

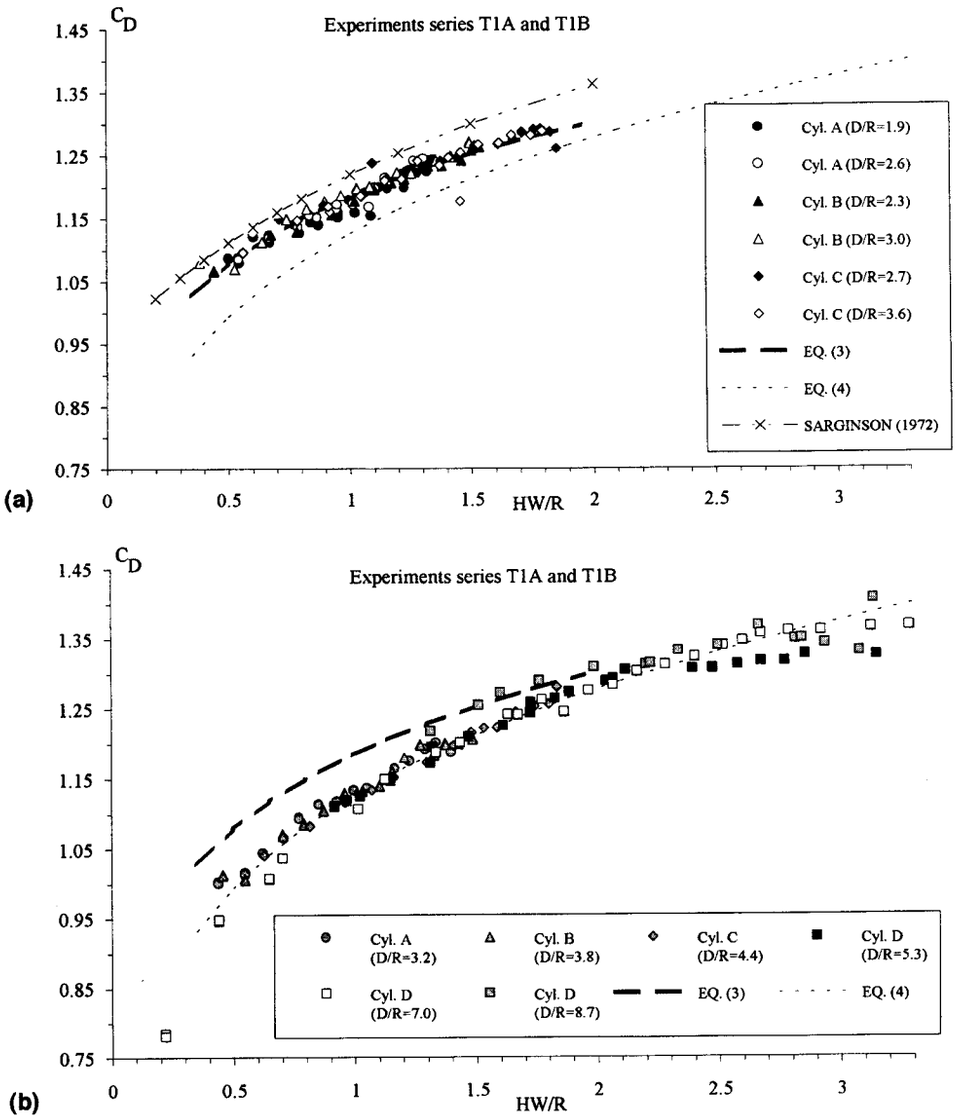

FIG. 4. Discharge Coefficient of Circular Cylinders: (a) Experimental Data for Fully Developed Inflow Conditions (Experiments Series T1A and T1B)—Comparison with Sarginson's (1972) Results; (b) Experimental Data for Partially Developed Inflow Conditions (Experiments Series T1A and T1B)

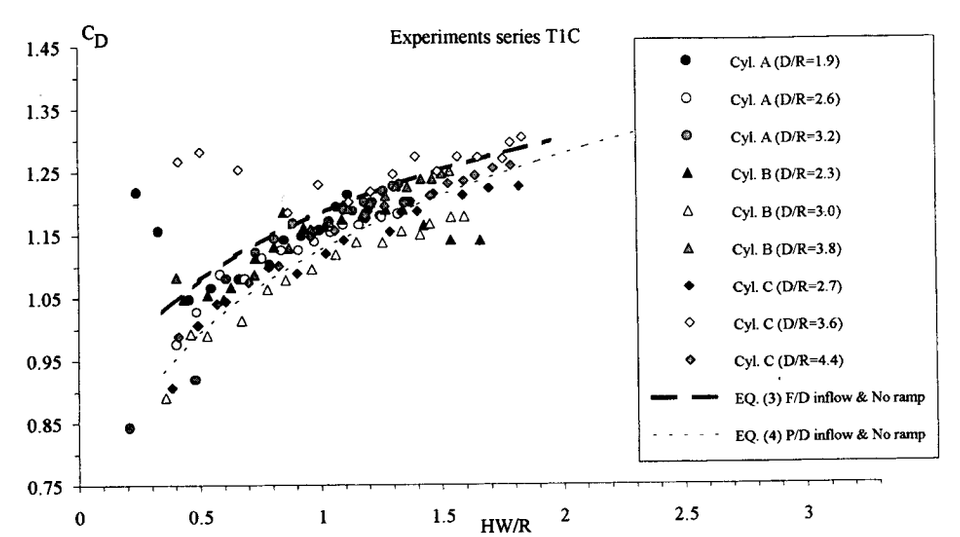

FIG. 5. Discharge Coefficient of Circular Cylinders: Effect of 30° Upstream Ramp. Comparison between Experimental Data with Upstream Ramp (Experiments Series T1C) and Eqs. (3) and (4) (No-Ramp Data)

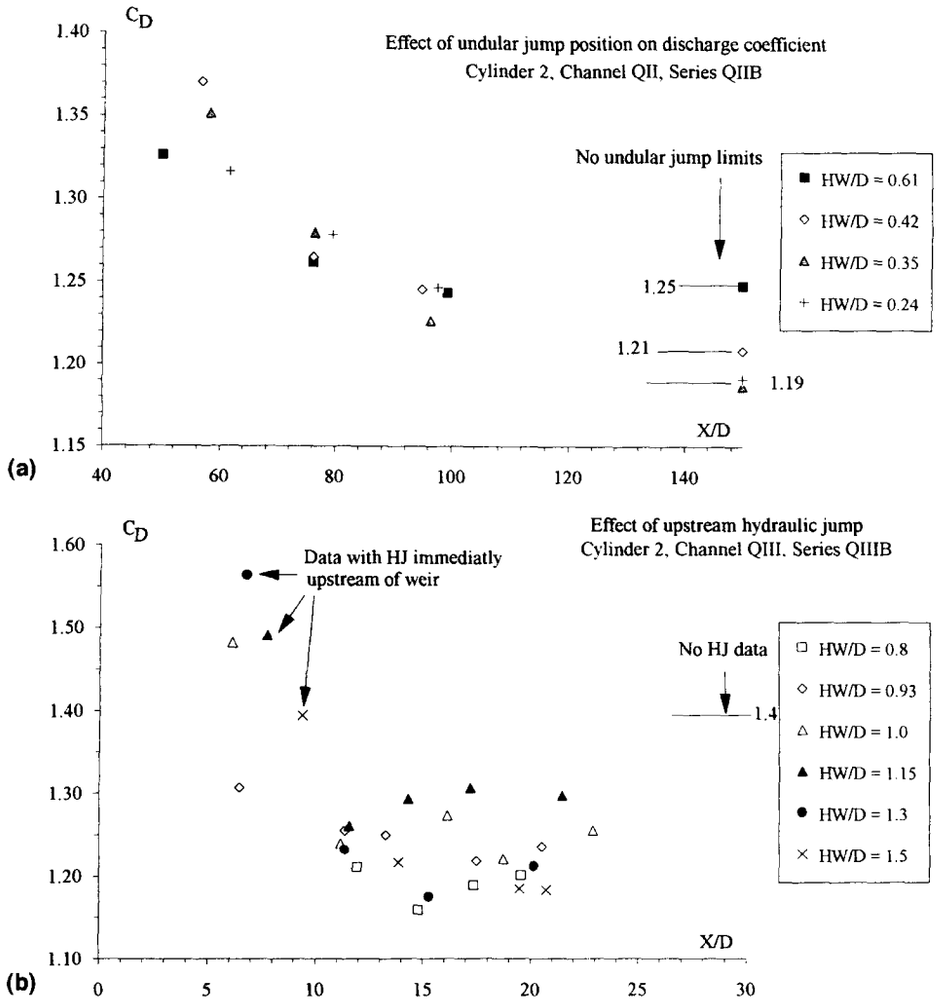

FIG. 6. Effect of Upstream Hydraulic Jumps on Cylindrical Weir Overflow: (a) Effect of Upstream Undular Jumps ($F \leq 1.25$)—C_D as Function of Dimensionless Distance of Jump (Experiments Series QIIB); (b) Effect of Breaking Hydraulic Jump (F between 3 and 10)—C_D as Function of Dimensionless Distance of Jump (Experiments Series QIIIB)

an undular hydraulic jump and the resulting free-surface undulations were observed to affect substantially the overflow pattern above the cylinders. The presence of a breaking hydraulic jump disturbs substantially the inflow, and such flow disturbances might explain the observed smaller discharge coefficients (than in absence of upstream hydraulic jump) [Fig. 6(b)]. When the normal hydraulic jump was located close to the weir (i.e., $X/D < 10$), the cylinder became engulfed into the jump roller and the flow over the cylinder became highly disturbed, although it still imposed a downstream control. Overall, these discharge coefficient data were not meaningful.

In summary, for a given ratio head on crest to curvature radius, the largest discharge coefficient is observed for inflow conditions with an upstream undular hydraulic jump and the smallest C_D is obtained for inflow conditions with an upstream (breaking) hydraulic jump.

Remarks

Although there is little information on the inflow conditions of past investigations (Fig. 3), one set of data (Sarginson 1972) was obtained with weirs placed at the end of a 20-m-long channel and the inflow conditions were fully developed. Fig. 4(a) shows a "relatively close" agreement between Sarginson's results and the present results for fully developed inflow conditions [(3)]. It is worth mentioning that Vo (1992) observed a maximum discharge coefficient for $HW/R \sim 5$ and, for larger ratios HW/R, C_D decreased and tended to sharp-crested weir values. These extreme flow conditions were not investigated in the present study.

Schoder and Turner (1929) investigated the effects of inflow conditions on sharp-crested weirs. Their results showed substantial modifications of the overflow characteristics when fences and screens were installed in the upstream channel to induce large bottom velocities or large free-surface velocities. Lindquist (1929) discussed these data, showing that the discharge coefficient was affected by the upstream flow conditions. In his analysis, Lindquist demonstrated that C_D was related to the kinetic energy correction coefficient of the upstream flow.

ANALYSIS

Flow Depth at Crest

In a rectangular horizontal channel with hydrostatic pressure distribution, the flow depth at critical flow conditions equals

$$d_c = \sqrt[3]{\frac{q_w^2}{g}} \tag{6}$$

d_c is commonly called the critical flow depth. At the crest of a cylindrical weir, critical flow occurs but the pressure distribution is not hydrostatic. The streamline curvature implies that the pressure gradient is less than hydrostatic and the velocity distribution is rapidly varied. For all these reasons, the flow

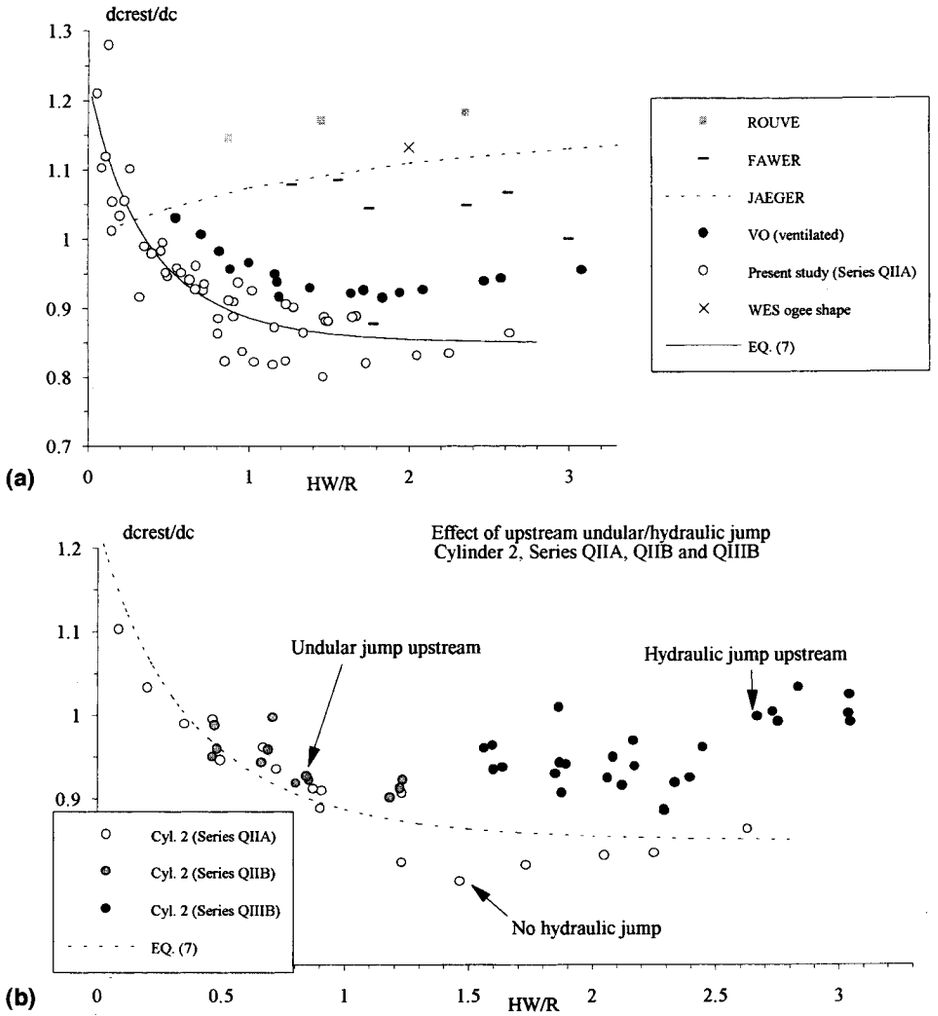

FIG. 7. Dimensionless Flow Depth at Crest of Circular Weirs: (a) Experimental Observations—Circular-Crested Weirs and WES Ogee Crest Weir (Present Data: Experiments Series QIIA, Cylinders 1, 2, 3, and 4); (b) Effect of Inflow Conditions on Flow Depth above Crest—Comparison between Fully Developed Inflows (Series QIIA), Upstream Undular Jumps (Series QIIB) and Upstream Hydraulic Jumps (Series QIIIB) for Cylinder No. 2 (R = 0.0524 m)

depth at the crest of circular cylindrical weirs is expected to differ from (6).

The flow depth at the crest was measured with cylinders 1 to 4. The results, reported in Fig. 7, indicate a decrease of the ratio of the flow depth at crest d_{crest} to critical depth d_c with increasing dimensionless upstream head on crest HW/R. For $HW/R > 0.4$ the flow depth at crest is smaller than d_c and, at large overflows ($HW/R > 0.8$), d_{crest}/d_c tends to a mean value of about 0.85. Overall, the data are best correlated by

$$\frac{d_{crest}}{d_c} = \frac{0.85}{1 - 0.31 \exp\left(-2.0 \frac{HW}{R}\right)} \quad \cdot 0.02 \leq HW/R \leq 2.63 \text{ and } 0.042 \leq R \leq 0.117 \text{ m} \qquad (7)$$

with a normalized correlation coefficient of 0.844 for a series of 110 data.

During the present study, the cylinder size R had no effect on dimensionless flow depth at crest d_{crest}/d_c. The type of inflow conditions (fully or partially developed) did not affect d_{crest}/d_c, and the presence of an upstream undular jump had little effect on the ratio d_{crest}/d_c. In the presence of an upstream (breaking) hydraulic jump, the flow depth at crest tends to be greater than without hydraulic jump, for a given upstream head above crest and discharge [Fig. 7(b)]. A careful analysis of the data showed no consistent trend between the breaking jump location and the flow depth at crest.

Fig. 7(a) includes also past experimental data and a reanalysis of Vo's (1992) data for $0.038 < R < 0.162$ m. In the same figure, the flow depth at the crest of a WES ogee-shaped weir (*Hydraulic* 1995) is shown for design flow conditions: $d_{crest}/d_c = 1.13$. Fig. 7(a) shows a substantial scatter between past and new data. Altogether it is worth noting the similar trend between the present work and the reanalysis of Vo's (1992) experiments. Although Vo's (1992) data were obtained with partially developed inflow conditions, both sets of data (the writers' and Vo's) indicate clearly that the ratio d_{crest}/d_c is less than unity for $HW/R > 0.5$. Note furthermore that the ratio d_{crest}/d_c is nearly constant for $HW/R > 1$: $d_{crest}/d_c \sim 0.85$ (writers) and $d_{crest}/d_c \sim 0.95$ (Vo). The different values might account for the difference of inflow conditions.

Energy Dissipation

The head loss at circular cylindrical weirs may be compared with the energy loss at a drop structure of same height (Fig. 8). Several researchers investigated experimentally the flow properties at drop structures. One (Chanson 1995, pp. 230–236) presented a detailed bibliographic review. Based on the experimental results of Rand (1955) (valid for $0.045 < d_c/D < 1$), he showed that the dimensionless head loss at a drop structure can be estimated as

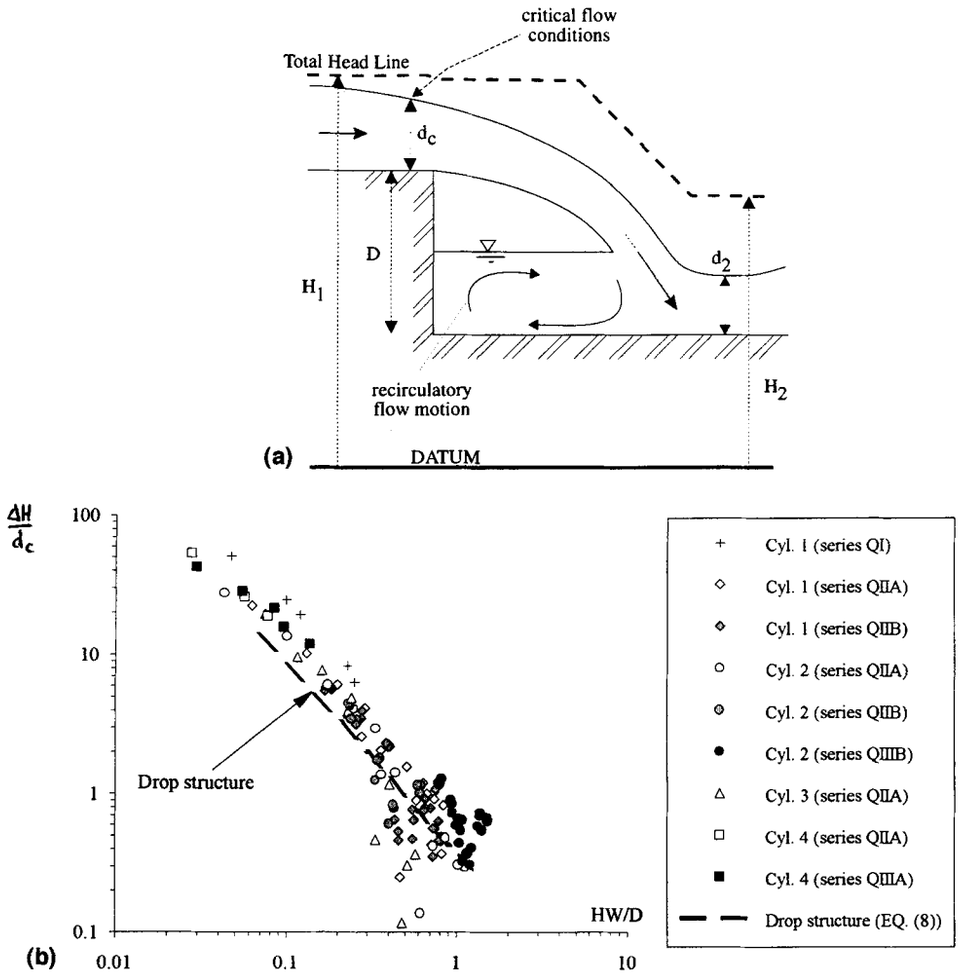

FIG. 8. Energy Dissipation Results: (a) Sketch of Drop Structure; (b) Dimensionless Head Loss $\Delta H/d_c$ as Function of Dimensionless Head on Crest *HW/D*—Comparison between Circular Cylindrical Weir Data (Series QI, QIIA, QIIB, QIIIA, and QIIIB) and Drop Structure Results [Eq. (8)]

$$\frac{\Delta H}{H_1} = 1 - \left(\frac{0.54 \left(\frac{d_c}{D}\right)^{0.275} + 1.71 \left(\frac{d_c}{D}\right)^{-0.55}}{1.5 + \frac{D}{d_c}} \right) \qquad (8)$$

where $\Delta H = H_1 - H_2$; H_1 = upstream total head [Fig. 7(a)]; D = drop height; and d_c = critical flow depth. Eq. (8) is compared with the experimental data in Fig. 8(b).

The data show a decrease in energy dissipation with increasing head on crest. At very low overflows (*HW/D* small), the head loss is nearly equal to the weir height D. For large overflows, the rate of energy dissipation becomes much smaller. Comparison between the data and (8) indicates basically that the dimensionless head loss is larger for a circular cylindrical weir than for a drop structure of same height and for a given head on crest.

Note the scatter of the data. The calculations of the downstream total head were not very accurate as the error on the flow depth measurement could be as large as 30%.

CONCLUSION

The writers investigated the overflow characteristics of circular weirs in the laboratory for a wide range of parameters: the cylinder radius (eight sizes), the weir height ($2 < D/R < 9$), the upstream flow conditions (upstream ramp, partially and fully developed inflow, upstream hydraulic jumps). No other experiments with extreme conditions of normal and undular jumps are available in the literature.

Experimental observations indicate that the overflow is characterized by nappe adherence on the downstream cylinder face and the overflow properties are significantly affected by the upstream flow conditions.

For the range of the experiments (Table 1), the writers observed that the cylinder size (i.e., radius of curvature R) has no effect on the discharge coefficient, dimensionless flow depth at crest, and dimensionless rate of energy dissipation. The dimensionless weir height D/R has no effect on the discharge coefficient. The presence of an upstream ramp has no effect on the discharge coefficient. The upstream flow conditions are extremely important and the type of inflow conditions affects substantially the overflow characteristics. For a given ratio head on crest to curvature radius, the largest discharge coefficient is observed for inflow conditions with an upstream undular hydraulic jump, and the smallest C_D is obtained for inflow conditions with an upstream (normal) hydraulic jump; discharge coefficients for partially and fully developed inflows are between the extremes.

The flow depth at the weir crest is usually lower than the critical depth (in rectangular channels) but for very low discharges (i.e., $HW/R < 0.4$). At large overflows ($HW/R > 0.8$), d_{crest}/d_c is typically about 0.85.

The energy dissipation at a circular weir is substantial and it is larger than at a drop structure for given inflow conditions.

The study suggests that discharge measurements with circular weirs are significantly affected by upstream flow conditions and to a small, even negligible, degree by the upstream geometry of the weir.

APPENDIX I. EFFECT OF UPSTREAM FLOW CONDITIONS ON DISCHARGE COEFFICIENT

Considering the overflow above a weir crest, apply the Bernoulli equation along the free-surface streamline between the upstream flow location and the crest:

$$d_1 + \frac{V_{max}^2}{2g} = D + d_{crest} + \frac{V_s^2}{2g} \quad (9)$$

where d_1 = upstream flow depth; D = weir height; V_{max} = upstream free-surface velocity; g = gravity constant; d_{crest} = flow depth on the crest; and V_s = free-surface velocity on the crest. Eq. (9) makes no assumption on the pressure distribution at the weir crest. Further, for a developing flow, the free-surface velocity is the free-stream velocity of the developing boundary layer.

Assuming that the velocity distribution in the bottom boundary layer follows a power law:

$$\frac{V}{V_{max}} = \left(\frac{y}{\delta}\right)^{1/N} \quad (10)$$

where δ = boundary layer thickness, the free-surface velocity can be derived from the continuity equation. Assume that the free-surface velocity at the weir crest equals

$$V_s = k\,\frac{q_w}{d_{crest}} \quad (11)$$

where k = constant of proportionality.

Combining the continuity and Bernoulli equations and using these assumptions [(10) and (11)], the discharge per unit width can be expressed as

$$q_w^2 = 2g\,\frac{d_1 - D - d_{crest}}{\dfrac{k^2}{d_{crest}^2} - \left\{\dfrac{N+1}{d_1^2[N+1-(\delta/d_1)]}\right\}^2} \quad (12)$$

Assuming that the discharge per unit width can be approximated as

$$q_w = C_D\sqrt{g}\left[\frac{2}{3}(H_1 - D)\right]^{3/2} \approx C_D\sqrt{g}\left[\frac{2}{3}(d_1 - D)\right]^{3/2} \quad (13)$$

where C_D = discharge coefficient; and H_1 = upstream total head, the discharge coefficient can be expressed as

$$C_D = \frac{d_{crest}}{d_c} \cdot \sqrt{\left[3\left(1 - \frac{2}{3}\frac{d_{crest}}{d_c}\right)\right] \Big/ \left\{k^2 - \frac{d_{crest}^2}{d_1^2}\left[\frac{N+1}{N+1-(\delta/d_1)}\right]^2\right\}} \quad (14)$$

Eq. (14) gives the expression of the discharge coefficient as a function of the ratios $d_{crest}/(d_1 - D)$, d_{crest}/d_1, and δ/d_1, and of the coefficients k and N. Present experiments indicate that the ratio d_{crest}/d_c is a function of the ratio head on crest to curvature radius, but they also suggest that it is nearly independent of the upstream flow conditions.

Note that the preceding results are general and may apply to most weir shapes.

ACKNOWLEDGMENTS

The writers thank M. Butterworth and R. O'Grady (University of Tasmania, Australia), and R. McConaghy and A. Swincer (University of Queensland, Australia) for their help and assistance. They thank also A. S. Ramamurthy (Concordia University, Canada) for providing the original data of his former PhD student (Vo 1992).

APPENDIX II. REFERENCES

Anwar, H. O. (1967). "Inflatable dams." *J. Hydr. Div.*, ASCE, 93(3), 99–119.

Bazin, H. (1888). "Expériences Nouvelles sur l'Ecoulement par Déversoir [recent experiments on the flow of water over weirs]." *Mémoires et Documents, Annales des Ponts et Chaussées*, Paris, France, Sér. 6, Vol. 16, 2nd Sem., 393–448 (in French).

Bazin, H. (1890). "Expériences Nouvelles sur l'Ecoulement par Déversoir [recent experiments on the flow of water over weirs]." *Mémoires et Documents, Annales des Ponts et Chaussées*, Paris, France, Sér. 6, Vol. 19, 1st Sem., 9–82 (in French).

Bazin, H. (1891). "Expériences Nouvelles sur l'Ecoulement par Déversoir [recent experiments on the flow of water over weirs]." *Mémoires et Documents, Annales des Ponts et Chaussées*, Paris, France, Sér. 7, Vol. 2, 2nd Sem., 445–520 (in French).

Bazin, H. (1894). "Expériences Nouvelles sur l'Ecoulement par Déversoir [recent experiments on the flow of water over weirs]." *Mémoires et Documents, Annales des Ponts et Chaussées*, Paris, France, Sér. 7, Vol. 7, 1st Sem., 249–357 (in French).

Bazin, H. (1896). "Expériences Nouvelles sur l'Ecoulement par Déversoir [recent experiments on the flow of water over weirs]." *Mémoires et Documents, Annales des Ponts et Chaussées*, Paris, France, Sér. 7, Vol. 12, 2nd Sem., 645–731 (in French).

Bazin, H. (1898). "Expériences Nouvelles sur l'Ecoulement par Déversoir [recent experiments on the flow of water over weirs]." *Mémoires et Documents, Annales des Ponts et Chaussées*, Paris, France, Sér. 7, Vol. 15, 2nd Sem., 151–264 (in French).

Belanger, J. B. (1828). "Essai sur la Solution Numérique de quelques Problèmes Relatifs au Mouvement Permanent des Eaux Courantes [essay on the numerical solution of some problems relative to steady flow of water]." *Carilian-Goeury*, Paris, France (in French).

Chanson, H. (1995). "Hydraulic design of stepped cascades, channels, weirs and spillways." *Pergamon*, Oxford, U.K., Jan.

Chanson, H. (1996). "Some hydraulic aspects during overflow above inflatable flexible membrane dam." *Rep. CH47/96*, Dept. of Civ. Engrg., University of Queensland, Australia, May.

Chanson, H., and Montes, J. S. (1997). "Overflow characteristics of cylindrical weirs." *Res. Rep. No. CE154*, Dept. of Civ. Engrg., University of Queensland, Australia.

Coanda, H. (1932). "Procédé de Propulsion dans un Fluide [propulsion process in a fluid]." *Brevet Invent. Gr. Cl. 2*, No. 762688, France (in French).

Creager, W. P. (1917). *Engineering of masonry dams*. John Wiley & Sons, Inc., New York, N.Y.

Escande, L., and Sananes, F. (1959). "Etudes des Seuils Déversants à Fente Aspiratrice [weirs with suction slots]." *Jl La Houille Blanche*, Dec., No. Special B, 892–902 (in French).

Fawer, C. (1937). "Etude de Quelques Ecoulements Permanents á Filets Courbes [study of some steady flows with curved streamlines]," Thesis, Lausanne, Switzerland, Imprimerie La Concorde (in French).

Hydraulic design of spillways. (1995). U.s. Army Corps of Engineers, ASCE.

Jaeger, C. (1956). *Engineering fluid mechanics*. Blackie & Son, Glascow, U.K.

Lindquist, E. G. W. (1929). "Precise weir measurements—discussion." *Trans.*, ASCE, 93, 1163–1176.

Matthew, G. D. (1963). "On the influence of curvature, surface tension and viscosity on flow over round-crested weirs." *Proc. Instn. Civ. Engrs.*, London, U.K., 25, 511–524.

Montes, J. S. (1964). "On the influence of curvature, surface tension and viscosity on flow over round-crested weirs. Discussion." *Proc. Instn. Civ. Engrs.*, London, U.K., 28, 562–563.

Petrikat, K. (1958). "Vibration tests on weirs and bottom gates." *Water Power*, 10, 52–57; 99–104; 147–149; 190–197.

Rand, W. (1955). "Flow geometry at straight drop spillways." *Proc.*, ASCE, 81(791), 1–13.

Rehbock, T. (1929). "The river hydraulic laboratory of the Technical University of Karlsruhe." *Hydraulic laboratory practice*, ASME, New York, N.Y., 111–242.

Rouve, G., and Indlekofer, H. (1974). "Abfluss über geradlinige Wehre mit halbkreissförmigem Überfallprofil [Discharge over straight weirs with semicylindrical crest]." *Der Bauingenieur*, 49(7), 250–256 (in German).

Sarginson, E. J. (1972). "The influence of surface tension on weir flow." *J. Hydr. Res.*, Delft, The Netherlands, 10(4), 431–446.

Schoder, E. W., and Turner, K. B. (1929). "Precise weir measurements." *Trans.*, ASCE, 93, 999–1110.

Scimemi, E. (1930). "Sulla Forma delle Vene Tracimanti [the form of flow over weirs]." *L'Energia Elettrica*, Milan, Italy, 7(4), 293–305 (in Italian).

Vo, N. D. (1992). "Characteristics of curvilinear flow past circular-crested weirs," PhD thesis, Concordia University, Montreal, Canada.

Wegmann, E. (1922). *The design and construction of dams*, 7th Ed., John Wiley & Sons, Inc., New York, N.Y.

APPENDIX III. NOTATION

The following symbols are used in this paper:

C_D = discharge coefficient [Eq. (2)];
D = 1—circular weir height (m); 2—drop height (m);
d_c = critical flow depth (m) assuming a hydrostatic pressure distribution and uniform velocity distribution. In a rectangular channel, $d_c = \sqrt[3]{q_w^2/g}$;
d_{crest} = flow depth (m) measured at the weir crest;
d_1 = flow depth (m) upstream of the weir;
F = Froude number of the upstream jump;
g = gravity constant = 9.80 m/s^2 in Brisbane, Australia;
H = total head (m);
HW = upstream total head (m) above crest = $H_1 - D$;
H_1 = total head (m) upstream of the weir;
H_2 = total head (m) downstream of the weir;
k = constant of proportionality (see Appendix I);
N = exponent of velocity distribution power law;
q_w = water discharge per unit width (m^2/s);
R = curvature radius (m) of crest;
W = channel width (m);
X = distance (m) between the hydraulic jump front and the weir = $x_{dam} - x_{jump}$;
x_{dam} = distance (m) from the channel intake of the cylindrical weir centerline;
x_{jump} = upstream position (m) of hydraulic jump measured from channel intake;
α = channel slope;
ΔH = head loss (m);
Δz = broad-crested weir height (m);
δ = boundary layer thickness (m);
ρ_w = water density (kg/m^3); and
σ = surface tension between air and water (N/m).

Subscripts

1 = flow conditions upstream of weir; and
2 = flow conditions downstream of weir.